Title

Climate sensitive size-dependent survival in tropical trees

Journal

Nature Ecology & Evolution, 2(9)

ISSN

2397-334X

Authors

Johnson, Daniel J

Needham, Jessica

Xu, Chonggang

et al.

Publication Date

2018-09-01

DOI

10.1038/s41559-018-0626-z

Peer reviewed

Climate sensitive size-dependent survival in tropical trees

Daniel J. Johnson [1,2]*, Jessica Needham[3] , Chonggang Xu[1] , Elias C. Massoud[4], Stuart J. Davies[5] , Kristina J. Anderson-Teixeira [6], Sarayudh Bunyavejchewin[7] , Jeffery Q. Chambers[8], Chia-Hao Chang-Yang[9] , Jyh-Min Chiang[10], George B. Chuyong[11], Richard Condit[12], Susan Cordell [13], Christine Fletcher[14], Christian P. Giardina[13], Thomas W. Giambelluca[15], Nimal Gunatilleke[16], Savitri Gunatilleke[16], Chang-Fu Hsieh[17], Stephen Hubbell[18], Faith Inman-Narahari[19], Abdul Rahman Kassim[14], Masatoshi Katabuchi[20], David Kenfack[5], Creighton M. Litton[19], Shawn Lum[21], Mohizah Mohamad[22], Musalmah Nasardin[14], Perry S. Ong [23], Rebecca Ostertag[24], Lawren Sack[25], Nathan G. Swenson[26], I Fang Sun [27], Sylvester Tan[22], Duncan W. Thomas[28], Jill Thompson[29], Maria Natalia Umaña[26], Maria Uriarte[30], Renato Valencia[31], Sandra Yap[32], Jess Zimmerman[33], Nate G. McDowell[34] and Sean M. McMahon[3]

1 Earth and Environmental Science, Los Alamos National Laboratory, Los Alamos, NM, USA. 2 School of Forest Resources and Conservation, Gainesville, FL, USA. 3 Forest Global Earth Observatory, Smithsonian Environmental Research Center, Edgewater, MD, USA. 4Department of Civil and Environmental Engineering, University of California, Irvine, CA, USA. 5 Forest Global Earth Observatory, Smithsonian Tropical Research Institute, Washington, DC, USA. 6Forest Global Earth Observatory, Smithsonian Conservation Biology Institute, Front Royal, VA, USA. 7 Research Office, Department of National Parks, Wildlife and Plant Conservation, Bangkok, Thailand. 8Climate and Ecosystems Science Division, Lawrence Berkeley National Laboratory, Berkeley, CA, USA. 9Department of Natural Resources and Environmental Studies, National Dong Hwa University, Hualien, Taiwan. 10Department of Life Science, Tunghai University, Taichung, Taiwan. 11Department of Botany and Plant Physiology, University of Buea, Buea, Cameroon. 12Field Museum, Chicago, IL, USA. 13Institute of Pacific Islands Forestry, USDA Forest Service, Hilo, HI, USA. 14Forest Research Institute Malaysia, Kepong, Selangor Darul Ehsan, Malaysia. 15Department of Geography, University of Hawai‘i at Mānoa, Honolulu, HI, USA. 16Department of Botany, University of Peradeniya, Peradeniya, Sri Lanka. 17Institute of Ecology and Evolutionary Biology, National Taiwan University, Taipei, Taiwan. 18Center for Tropical Forest Science-Forest Global Earth Observatory, Smithsonian Tropical Research Institute, Panama, Republic of Panama. 19Department of Natural Resources and Environmental Management, University of Hawaii at Manoa, Honolulu, HI, USA. 20Department of Agricultural and Biological Engineering, University of Florida, Gainesville, FL, USA. 21Nanyang Technological University, Singapore, Singapore. 22Sarawak Forestry Department, Kuching, Sarawak, Malaysia. 23Institute of Biology, University of the Philippines Diliman, Quezon City, Philippines. 24Department of Biology, University of Hawaii, Hilo, HI, USA. 25Department of Ecology and Evolutionary Biology, University of California, Los Angeles, Los Angeles, CA, USA. 26Department of Biology, University of Maryland, Baltimore, MD, USA. 27National Dong Hwa University, Hualian, Taiwan. 28School of Biological

Sciences, Washington State University, Vancouver, WA, USA. 29Centre for Ecology & Hydrology, Bush Estate, Penicuik, Midlothian, UK. 30Department of Ecology, Evolution & Environmental Biology, Columbia University, New York, NY, USA. 31Escuela de Ciencias Biológicas, Pontificia Universidad Católica del Ecuador, Quito, Ecuador. 32Far Eastern University, Manila, Philippines. 33Institute for Tropical Ecosystem Studies, College of Natural Sciences, University of Puerto Rico, Río Piedras, Puerto Rico. 34Pacific Northwest National Laboratory, Richland, WA, USA. *e-mail: johnson.daniel@ufl.edu

Abstract

Survival rates of large trees determine forest biomass dynamics. Survival rates of small trees have been linked to mechanisms that maintain biodiversity across tropical forests. How species survival rates change with size offers insight into the links between biodiversity and ecosystem function across tropical forests. We tested patterns of size-dependent tree survival across the tropics using data from 1,781 species and over 2 million individuals to assess whether tropical forests can be characterized by size-dependent life-history survival strategies. We found that species were classifiable into four ‘survival modes’ that explain life-history variation that shapes carbon cycling and the relative abundance within forests. Frequently collected functional traits, such as wood density, leaf mass per area and seed mass, were not generally predictive of the survival modes of species. Mean annual temperature and cumulative water deficit predicted the proportion of biomass of survival modes, indicating important links between evolutionary strategies, climate and carbon cycling. The application of survival modes in demographic simulations predicted biomass change across forest sites. Our results reveal globally identifiable size-dependent survival strategies that differ across diverse systems in a consistent way. The abundance of survival modes and interaction with climate ultimately determine forest structure, carbon storage in biomass and future forest trajectories.

Main

Tropical forests store an estimated 500–1,000 Pg of carbon in biomass and soils[1,2], making this biome the most important component of the terrestrial carbon cycle. Whether intact tropical forests will be sinks or sources of carbon in the future remains a critical question[1,3] that will fundamentally depend on how different forest species respond to climate change[4]. The high species diversity of tropical forests may either buffer stands from shifts in standing biomass or promote changes due to the characteristics of the species that best tolerate novel climate conditions. Forest carbon volume depends exponentially on the annual rate of tree survival, and tree survival rates in turn depend on climate[5] and a given species tolerance of climate variation. Most forests include short-lived species that die within decades to long-lived species that retain carbon for centuries. Species may be differentially vulnerable to novel climate variation or new regimes of

extreme episodic events (for example, droughts and storms). Resulting changes in forest composition may cause large and rapid changes in the terrestrial carbon balance that could potentially persist for centuries. Climate-driven impacts on tree survival are potentially more important than impacts on forest productivity (that is, photosynthesis and allocation to growth), which has a relatively constrained and slower influence on forest carbon dynamics[6,7,8,9].

For species to coexist in diverse forests, they must have roughly equivalent fitness over long time periods[10,11], yet differences in achieving that fitness can influence compositional shifts under novel long-term ecological changes. Tree species have evolved resource allocation strategies that, over the course of their life-history, variously emphasize investment in metabolic maintenance or in tissues that provide structural, defensive and reproductive functions. Diversity in resource allocation therefore scales up to variation in demographic rates (that is, survival, growth and reproduction). The survival rates that emerge from allocation to maintenance, defence and structure can then determine observed population distributions across space[12], size and age structures[13]. Allocation to tissues that increase survival are typically negatively correlated (or exhibit trade-off) with allocation to tissues involved in other demographic rates[14]. For example, using resources to build defensive structures reduces the resources available for growth. Conversely, allocation to tissues for increased growth can lead to distinct vulnerability to agents of mortality, such as pathogens[15], pests, storms, drought or extreme temperatures[16]. Trade-offs among life-history strategies should be reflected in variations in plant functional traits, which provide one way of classifying species into groups. Tolerance of various climate stressors may vary with allocation strategies, resulting in important implications for forest biodiversity and stocks. A greater understanding of how demographic rates vary with size should increase our ability to predict how diverse forests cycle carbon and provide insights into potential shifts in those cycles.

Here, we analyse variations in tree survival to provide a deeper understanding of basic ecological and evolutionary features of tropical forests. Using an exemplary dataset of more than 2 million trees across the tropics, we developed statistical models of size-dependent survival. Using a cluster analysis, we aggregated the results of these models into groups of similar survival strategies that we call ‘survival modes’ and analyse their relation to functional traits and climate and their ecological significance. First, we investigated how survival modes contribute to carbon fluxes through differences in growth rates and biomass turnover. Then we examined whether the modes of survival that emerge from the demographic data are related to the commonly collected plant traits of wood density, leaf mass per area (LMA) and seed mass. We also tested whether the relative abundance of these survival modes relate to climate

variables and tested the ability of survival mode relative abundance to predict observed biomass dynamics at each site through time.

Results

Survival models were fit for 1,781 species from 14 pan-tropical large-area forest dynamics plots that are all part of the ForestGEO network[17](ranging from 2 to 52 ha, each with 371 ha in total in which all stems ≥1 cm diameter at breast height are recorded; Supplementary Table 1). The parameters from these models were included in a principal component analysis (PCA) (Fig. 1 details the workflow; Supplementary Table 2summarizes the survival curve parameters). The PCA revealed axes of evolved life-history variation (Supplementary Figs. 1,2). For example, PCA axis one defined a continuum characterized by relatively stable survival probability, either high or low survival, across the life-cycle at one extreme and at the other extreme by increases and decreases in survival probability with size at small and large sizes. That is, species with more extreme thinning due to competition for resources when relatively small, or mortality causes related to large size and exposure to agents of mortality in the other direction[18]. Axis two differentiated species based on maximum survival rate (that is, the upper asymptote of the survival curve; Fig. 2).

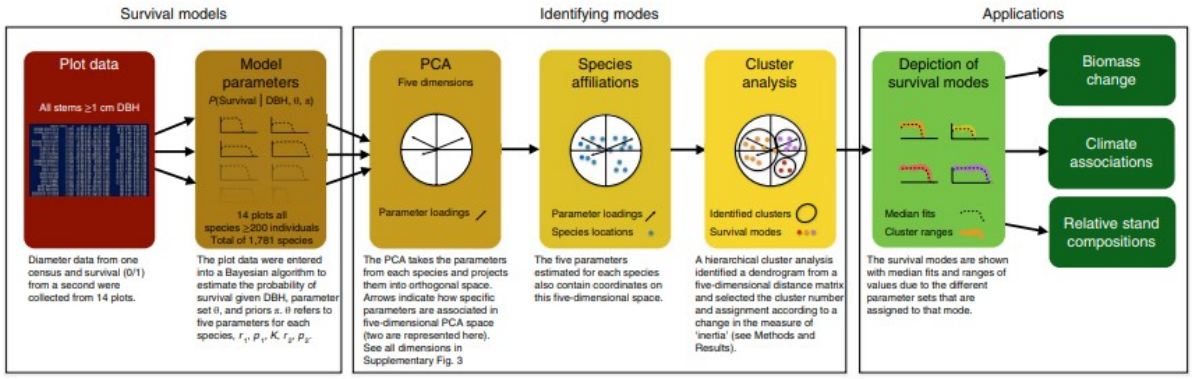

Fig. 1 | Schematic of the workflow for this analysis. Processes that were used to go from raw plot data to testing the implications of emergent survival modes.

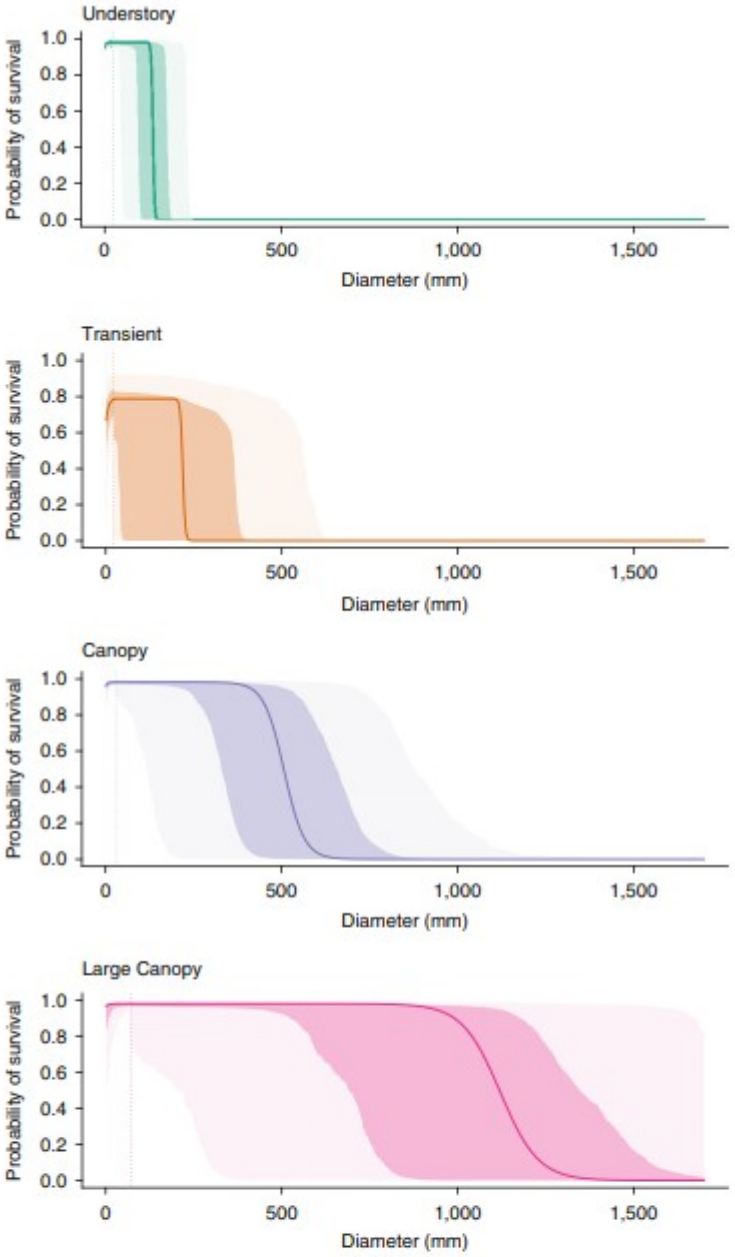

Fig. 2 | Survival probability as a function of DBH for each of the four identified survival modes. Survival modes were derived from a hierarchical cluster analysis on the parameters from the survival function fit to 1,781 species at 14 large-area forest plots. In each species, the survival function consists of two curves fit to individuals above and below a species-specific size threshold. The means of the size thresholds for species within each mode are shown as vertical broken lines. In each mode, the unbroken line represents the mean of the survival functions from species within the mode, and the light and dark shaded regions show the 50% and 90% uncertainty range around the mean. Parameters for each mean curve are listed in Supplementary Table 2.

Species survival curve parameters were hierarchically clustered by loadings of the PCA analysis, which creates a dendrogram from a similarity matrix, to find groups of species that were similar in size-dependent survival rates. An optimizing analysis across the dendrogram resolved four survival modes (Fig. 2; Methods). To test the robustness of our survival modes, we bootstrapped the Jaccard similarity index for all clusters that were substantially above the 0.75 threshold[19], which indicates stable clustering for our size-dependent survival modes (Supplementary Table 2). We utilized these four survival modes in subsequent analyses of traits, climate and carbon dynamics in tropical forests.

Although annual survival probability across much of the life cycle was high for most species (>0.95), there were species with much lower maximum survival rates (<0.78; Supplementary Table 2). Furthermore, the degree of small stature mortality varied between modes, indicating differences in the strength of mortality mechanisms in small sizes across the four modes. Finally, there were also clear differences in the maximum sizes; that is, the diameter beyond which species showed increased mortality, indicating important mode-dependent life expectancies (Fig. 2).

The four survival modes clustered along multiple principal component axes. However, species within clusters tended to have similar life forms; that is, the size at which mortality occurred was similar. Understory species are characterized by small maximum diameters, with an across-site mean 99th percentile diameter of 9.8 ± 2.4 cm (mean $\pm$ 1 s.d.). Transient species were distinguished by their very low overall survival with an across-site mean maximum-survival rate of 78% per year and an across-site mean 99th percentile diameter of 14.3 ± 9.4 cm. There were two groups of large stature tree species or species capable of reaching canopy sizes. Canopy species were the group with low small-diameter survival rates, intermediate maximum size and an across-site mean 99th percentile diameter of 27.8 ± 7.0 cm. Large Canopy species have relatively higher survival at smaller diameters and larger maximum diameter (68.4 ± 18.5 cm). Our analysis had an abundance threshold of 200 individuals; species with lower abundance were not included and are therefore Unclassified. However, we cannot exclude the possibility that some of them displayed other survival modes too rare to describe statistically.

Survival modes varied in abundance (Fig. 3) and diversity among forested plots (Fig. 3). The species included in the cluster analysis represented 76.7% (range, 46.9–97.0%) of the biomass on average across the plots (Supplementary Table 3; Supplementary Fig. 3). The Canopy mode was typically the most species-rich, followed by the Understory and Large Canopy modes (Supplementary Table 4).

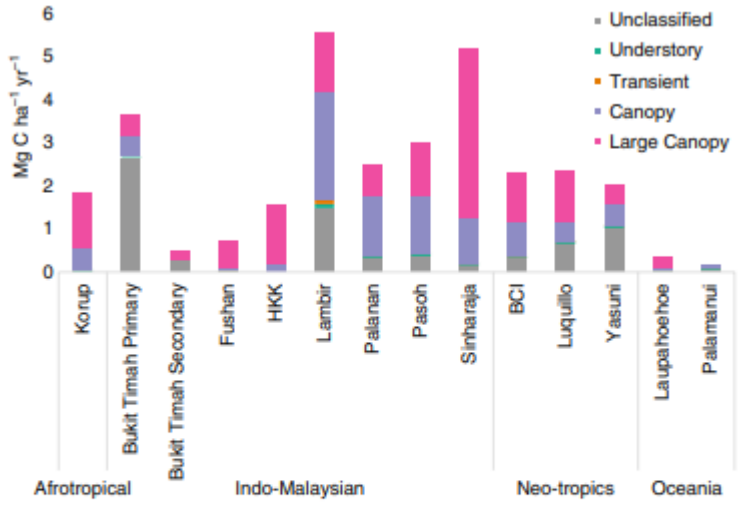

Fig. 3 | Mean annual aboveground carbon loss to mortality. Site-level mean annual aboveground carbon loss to mortality for each survival mode across all census intervals. Species that did not have enough individuals to model survival are presented as Unclassified. Corollary figures for mortality rates are presented in Supplementary Fig. 10. HKK, Huai Kha Khaeng; BCI, Barro Colorado Island.

We calculated carbon lost to mortality at each site to understand the influence of these survival modes on carbon residence times. Total carbon loss from tree mortality ranged from 0.14 Mg C ha^{-1} yr^{-1} at the dry tropical forest Palamanui plot in Hawaii to 5.6 Mg C ha^{-1} yr^{-1} at Lambir, Malaysia, with a mean of 2.28 Mg C ha^{-1} yr^{-1} for all survival modes, including Unclassified (Fig. 3). Surprisingly, the plots that are commonly struck by typhoons and hurricanes (Fushan, Luquillo and Palanan) had intermediate rates of carbon loss due to mortality even though the plots experienced storms during sampled intervals. This result demonstrates that species at these sites have potentially been selected to tolerate disturbances instead of recover from them. The overall proportion of carbon lost to mortality varied greatly among these forests, although on average, Indo-Malaysian forests had the highest rates of absolute carbon loss (Fig. 3). Conversely, relative to total biomass, neo-tropical forests lost slightly more biomass (Supplementary Table 3). Relative proportions of biomass lost to mortality ranged from 0.02 to 9.5% for Understory mode species, 0 to 0.4% for Transient mode species, 1.3 to 85.2% for Canopy mode species and 1.6–61.8% for Large Canopy species.

Commonly measured plant functional traits had only limited ability to predict survival modes, which is due to the diversity among species within given survival modes in these traits. Across all sites, the Transient mode species had significantly less dense wood than the other survival modes ($F = 9.65$, $P < 0.001$ (analysis of variance (ANOVA)); Fig. 4a). When we limited the analysis to sites (7 of 14) that had locally collected wood density values, the Large Canopy and the Transient groups both had significantly

lower wood density than the Understory and Canopy survival modes (Supplementary Fig. 4). In parallel with wood density, the Transient and Large Canopy species had significantly lower LMA than the Understory and Canopy species ($F = 7.28$, $P < 0.001$ (ANOVA); Fig. 4b). Seed mass did not differ significantly among survival modes ($F = 2.26$ for log-transformed data, $P = 0.086$ (ANOVA); Fig. 4c). These analyses were constrained by the limited availability of functional trait data, whereby LMA was only available for 40.4% and seed mass for only 8.1% of species.

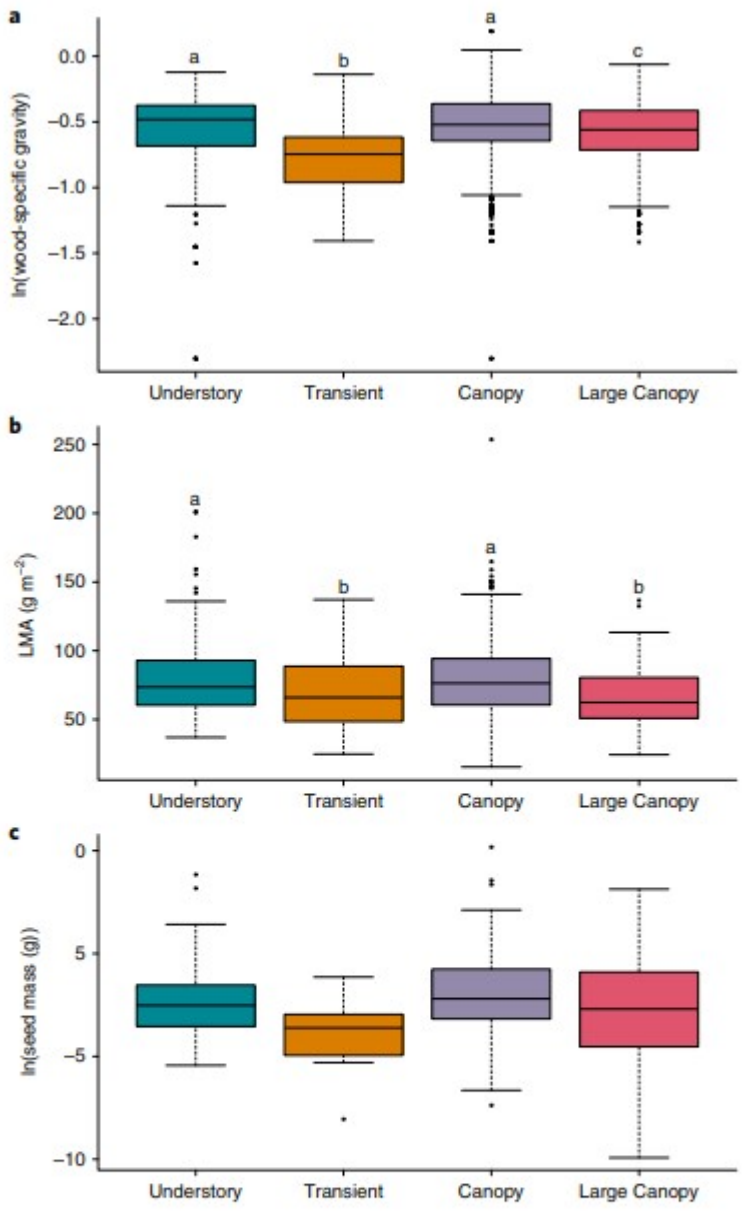

Fig. 4 | In general, traits do not map strongly onto the four survival modes. a, Natural log-transformed wood-specific gravity at all sites. **b**, LMA at six sites (Lambir, BCI, Luquillo, Laupahoehoe, Palamanui and Fushan). **c**, Natural log-transformed seed mass and survival modes at Luquillo, Laupahoehoe, Palamanui and BCI where there were no significant differences between survival modes. Whiskers on boxes indicate the range of the data out to 1.5 times the length of the box. Letters represent significant differences among survival modes in traits at alpha = 0.05 by Tukey HSD test.

We related mean annual temperature (MAT), mean annual precipitation (MAP) and cumulative water deficit (CWD) at each forest to the relative percentage biomass of survival modes (Supplementary Fig. 5) to understand whether there were climate dependencies in survival mode

composition. Multiple linear Tobit regression indicated that Large Canopy biomass relative abundance had a negative relation to MAT, a positive relation to CWD and no relation to MAP ($P = 0.000083$, McFadden's[20] pseudo $R^2 = 0.24$; note that this is not the same as ordinary least squares R^2, and a model with a statistically good fit to the data will have McFadden's pseudo R^2 value between 0.2 and 0.4). The relative percentage biomass of Canopy and Large Canopy survival modes were strongly inversely related (Supplementary Fig. 3). Transient survival mode biomass was negligible and was not modelled. The Understory mode relative biomass was positively related to MAT ($P = 0.031$, McFadden's pseudo $R^2 = 0.12$), but lacked any significant relation to CWD or MAP.

To clarify how survival and growth interact to affect the progression of individuals through their life cycle, we calculated mean growth rates by survival mode. Growth rates significantly differed among survival modes, whereby the Large Canopy survival mode had the largest mean annual diameter growth rate $2.18\,\mathrm{mm\,yr^{-1}}$. Conversely, the Understory survival mode was the slowest growing at $0.52\,\mathrm{mm\,yr^{-1}}$ (Fig. 5). A similar pattern was found when growth was expressed in terms of biomass accumulation (Supplementary Fig. 6). The Canopy mode has nearly half the growth rate of the Large Canopy mode, suggesting that carbon residence times of these two groups may be similar, but the Large Canopy mode would sequester more carbon in a similar time frame.

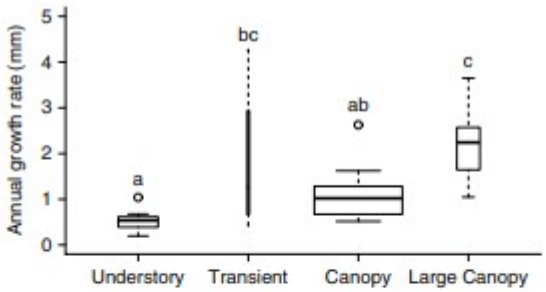

Fig. 5 | Average annual individual growth rate by survival mode. Plot-level average annual individual growth rate by survival mode boxplots with the width scaled to the square-root of the number of species that make up the survival mode for all forest plots. Whiskers on boxes indicate the range of the data out to 1.5 times the length of the box. Significant differences ($n = 14$, alpha = 0.5, Tukey HSD test) are denoted by letters above survival mode.

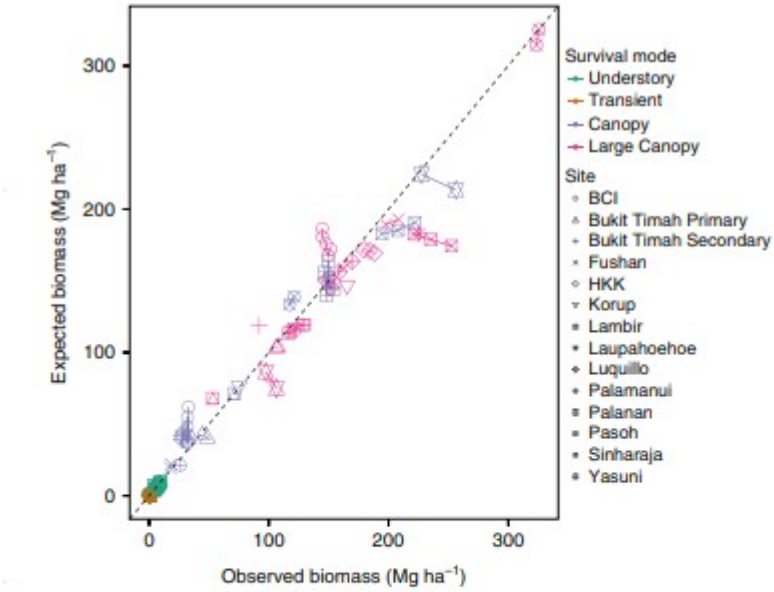

Fig. 6 | Observed versus predicted biomass. Observed biomass by survival mode versus predicted biomass from an individual based model at each site (marginal $R^2 = 0.9735$). The line between points traces census interval typically diverging from the broken line, which represents the 1:1 line, with time.

We tested the ability of survival mode composition to predict whole-forest biomass in simulations. We found a strong correlation (marginal $R^2 = 0.97$) between the observed biomass in each survival mode and the biomass predicted from an individual based model (IBM) run at each site, in which individuals were classified only by their survival mode (Fig. 6). Biomass was relatively small and changed little across census intervals for the Understory and Transient survival modes. The accuracy of predictions of biomass varied for the Large Canopy and Canopy modes. Predicted

biomass was underestimated for the Large Canopy mode at Lambir and Laupahoehoe by 47.68 and 42.15 Mg ha^{-1}, respectively. In contrast, expected biomass was overestimated by the IBM for the Canopy and Large Canopy modes at Barro Colorado Island (BCI) by 14.45 and 26.62 Mg ha^{-1}, respectively.

Discussion

Our results provide objective and quantitative descriptions of global size-dependent tropical tree survival that reflect some of the classical descriptors of tree species demographics[21]. We discovered groups of species that differ in how they survive as they grow and that the probability of survival at small sizes varied among the survival modes. This result was derived from our classification of size-dependent survival curves and are likely to reflect the trade-offs inherent in competition for limited resources (for example, light) in the understory[22] or to susceptibility to pests[23] and pathogens[24,25]. We also found that survival modes varied in large-sized mortality, in which causes of mortality are likely to be driven by the reallocation of resources from resistance to or tolerance of structural damage[26], water limitation[16] and accumulation of pathogens[27] and other factors[18]. Our contention that this difference in survival at large sizes is a life-history strategy and not simply a product of a lower average survival rate for earlier senescing modes. This contention is supported by the fact that three of the four modes had very similar maximum survival rates, but differed remarkably in their size at senescence.

Past studies have indicated that tree survival under environmental stress can depend on tree size[16,28]. We discovered that climatic factors correlated well with the relative biomass of survival modes across forests, indicating that climatic factors may influence forest composition. Because the climate correlates with different proportions of survival modes suggests that there are differences in carbon residence times and forest structure with climate. Higher relative biomass in the Large Canopy survival mode was observed in forests with lower MAT and longer dry seasons and less Canopy species biomass. Considering that larger individuals can be more susceptible to drought[16], the CWD result seems counter-intuitive at first. However, drought and seasonally dry climate differ in their effects on large trees, with large trees in seasonally dry climates being adapted to dry seasons[29]. Additionally, the prevalence of the Large Canopy mode may be influenced by environmental factors not considered here, such as soils or biogeographical history. Differences in the dominance of survival modes among tropical forests are likely to be driven by many mechanisms, and understanding the drivers is an important next step towards accurately forecasting the fate of forests[18].

Widely collected plant traits explained some of the differences in size-dependent survival modes in our analysis. Wood density has been recognized as a significant predictor of tree survival[30,31] and of growth

survival trade-off in saplings[32], but variation in size-dependent survival was not explicitly considered in the studies. We found that a clear difference between wood density means and survival modes for the Transient mode, which is likely to describe aggressive light-dependent pioneering species. Lower LMA in the Transient and Large Canopy modes combined with higher mean growth rates suggests that the species in these survival modes probably have higher metabolic costs, potentially higher leaf nitrogen concentrations and shorter life leaf-span[33]. Variation in seed mass may reflect a suite of strategies independent from allocation to size-dependent survival at the sizes we examined. Seed mass might correlate better with individual growth rates or with different the reproduction life-history strategies of species[34]. Alternatively, seed mass may correlate with survival in individuals <1 cm diameter at breast height (DBH), which was not measured in our analysis. The variation in traits observed within survival modes suggests that survival is a key demographic axis to examine because trait variation is one condition for the coexistence of diverse species[35]. Overall, our results suggest that a greater variety of traits and measurement of traits in each forest could advance our understanding of the links between tree performance and tree functional traits.

Our IBM model predictions provided a good fit to the observed forest biomass. Despite large amounts of demographic data being available globally, few studies have moved beyond descriptions of mortality averaged over species or coarse size classes. Models in which survival probability changes as a continuous function of size are necessary to accurately represent the variation in the way that individuals of different species move through the life cycle. Such models will therefore allow more biologically nuanced forward projection of populations and communities. Even when combined with a relatively simple growth model, the average parameters from our survival modes were able to capture the change in biomass at each site attributed to each survival mode.

The IBM projections demonstrated that our survival modes can provide benchmarks for biome models that simulate forest dynamics at a global scale (for example, terrestrial biome models (TBMs) or dynamic global vegetation models (DGVMs)), whereby vegetation is coupled with climate. Attempts at modelling carbon fluxes in DGVMs have led to very divergent results due to the potential response of forests, both in estimates of future atmospheric carbon[36] and in terrestrial vegetation carbon stocks[6]. The evolutionary strategies of tree survival, integrated within the ecological models of environmental conditions, might provide a better pathway towards forecasting these diverse systems[6,37]. To do so, however, requires integration of field data, statistical models and size-structured TBMs that can accept demographic data as inputs. In a post hoc analysis, we compared the observed mortality rates from our plot data with mortality rates from one size-structured DGVM, functionally assembled terrestrial ecosystem simulator (FATES), using simulation results of one tropical

broadleaf evergreen plant functional type and climate drivers from a one degree area of the Amazon (E. C. Massoud et al., manuscript in preparation). We found that FATES underestimated small-diameter tree survival but overestimated large-diameter tree survival compared with our results. Specifically, the annual mortality rate of trees larger than 70 cm DBH in FATES was 1.47%, while the observed mean annual mortality rate from ForestGEO plots for the same size class was 2.85% (Supplementary Fig. 7), which could result in overestimation of carbon storage in the FATES model. This deviation from the FATES model is not a large difference; however, mortality rates compound annually, and this almost twofold underestimate of annual mortality reflects a significant mismatch in the pace of forest dynamics over decades. Although this is only a simple comparison with one model, it indicates a way in which demographic data can be aggregated into life-history strategies, which in turn can provide benchmarks to assess vegetation model performance. Incorporation of size-dependent survival constraints, for example, could improve how we assess, and perhaps how we model, mortality for the suite of DGVMs that are able to incorporate size-based survival[38].

Despite the large range of species diversity and biomass turnover represented in our analysis, we found consistent patterns of size-dependent survival (Supplementary Fig. 8) that are not strongly tied to commonly collected plant traits. The relative abundance of different survival modes varied with temperature and water deficit, which has implications for community composition, dynamics and carbon storage. If the temperature–survival mode relation is mechanistically driven, then forests would shift from dominance by Large Canopy mode species to Canopy mode species as temperature rise, resulting in less carbon sequestered. Future work based on our findings should investigate how trade-offs in growth and survival affect the survival modes identified, and how forecasting tropical carbon stocks could be improved by explicitly considering large-tree survival mechanism to constrain terrestrial carbon dynamics.

Methods

We used a global dataset of tree demography to build models of survival probability as a function of size. We used data from 14 plots that follow the same methodology: all woody stems ≥1 cm DBH have been identified to species, mapped and measured every 5 years (following that of a previous study[39] and summarized in Supplementary Table 1). All species with >200 observations across the censuses were included in the following analyses, comprising a total sample of over 2 million individuals in 1,781 species. All analyses were conducted in R package[40].

We estimated size-dependent survival by fitting a functional form to the data for every species in each census interval (see Fig.1 for a workflow diagram). We used a Bayesian framework (see Supplementary Table 5 for

details of model fitting) and fit the model in R using Stan[41], a platform for statistical modelling. The basic form of the survival function allows for variations in the classic U-shaped mortality curve[13,42,43,44] (ours is inverted to survival). Because the data are heavily weighted to small individuals and the mechanisms that cause mortality across size can vary significantly, we combined two logistical functions to describe tree survival across size: one function to describe survival at small sizes and one for larger sizes[45] (see Supplementary Fig. 8 for examples of the species-specific fits and Supplementary Fig. 9 for sites). The probability of survival is therefore given by the following equation:

$$S = \left(\frac{K}{1 + e^{(-r_1((x - p_1)))}} \right)^t \text{ for all } x < \text{thresh (small sizes)} \quad (1)$$

$$S = \left(\frac{K}{1 + e^{(-r_2((x - p_2)))}} \right)^t \text{ for all } x \geq \text{thresh (large sizes)}$$

where S is survival probability across the census interval, K, r and p are the upper asymptote, the rate of change and the inflection point of the survival curve, respectively, x is size (DBH in mm), t is the time in years between censuses, and thresh is the size threshold at which the two functions meet. The threshold was set at the median DBH size (see Supplementary Fig. 8) to ensure that each species had an equal number of observations informing each of the two curves. Subscripts 1 and 2 denote parameters for the curves describing survival in individuals below and above the size threshold, respectively.

The parameters in these functions hold distinct meanings across tree life-history. K determines the maximum annual survival probability and usually remains constant over most of the life history of a tree. Mortality of small individuals, often due to thinning in the understory, is determined by r_1 and p_1. Their complementary parameters for the large function r_2 and p_2 define survival at the largest sizes and may indicate the maximum size observed for a species.

The five parameters from the joint survival functions (K, r_1, p_1, r_2 and p_2) for each species in each census interval were included in a PCA to remove correlations among parameters and to find the orthogonal axes of variation in survival strategies throughout the life cycle, with all parameters standardized to unit scale. To ensure that species from each site carried equivalent information in the PCA, species were weighted equal to the inverse of the number of census intervals over which they were modelled.

In order to group species into survival strategies, we derived survival modes based on species position in the PCA space that describe the greatest variation in species survival through the life cycle. We selected clusters based on the following three criteria: the statistical metric that identified significant separation of groups of species in PCA space; a

qualitative meaning to these clusters that could be mapped to survival strategies known to exist among forest tree species; and survival modes that could inform forest dynamics based on their contribution to different forest types.

Hierarchical cluster analysis was performed on the first five dimensions of the PCA using the hierarchical clustering on principal components (HCPC) function from the R package FactoMineR[46]. The HCPC function builds a dendrogram of species survival similarity from a similarity matrix. It then calculates the within- and between-group sum of squares (also termed inertia) for a range of potential cluster numbers and selects the number of clusters for which the change in between group variance is minimized[47]. Four clusters were selected using this algorithm, and we tested the robustness of the recommended clusters with the Jaccard similarity index produced via the bootstrapping function clusterboot in the fpc package[19]. Along with being statistically robust, these clusters describe observed life-history strategies. That is, the mean survival curve for each mode matches the observed size-dependent survival patterns (Fig. 2 and Supplementary Fig. 8). We used the mean values of parameter sets within each cluster (from the survival function fits) and their covariances to randomly draw 1,000 simulated survival curves. At each millimetre increment, from one to the maximum size, we then selected the mean, 50% and 90% quantile values. We also plotted the survival function corresponding to the most representative species of each mode (Supplementary Fig. 9); that is, the species from each cluster closest to the centroid.

In calculations of biomass or carbon loss due to mortality for each survival mode, biomass was calculated for the main stem of each tree using general tropical allometries for trees without height measurements[48], as tree height measurements are not part of the ForestGEO monitoring protocol. These allometries estimate height based on the diameter of the stem and an environmental index to estimate biomass. For each survival mode, annual carbon loss (half of biomass loss) due to mortality was based on the tree diameter at the beginning of the census interval and made to be annual by dividing by the mean census interval time (typically ~5 years). We, also report mean mortality rate by survival mode at each site for comparability to other studies (Supplementary Fig. 10). Absolute annual diameter growth rates were calculated for each survival mode by subtracting diameters at the beginning of the census interval from the ending diameter and dividing by the time between censuses for each tree.

We tested the correlation between survival modes and the following three common functional traits: wood density, LMA and seed mass. Trait values for wood density ($n = 1{,}781$, some species were assigned genus or family level values when species-specific values were not available) were obtained from compiled databases[49,50,51], and half of the plots had locally collected wood density values. LMA ($n = 719$) and seed mass ($n = 144$) data were collected locally[32,52] (Sack et al., unpublished observations, and Sack

and Yoshinaga, unpublished observations). Differences between trait means among survival modes were compared using ANOVA with Tukey HSD tests for multiple comparisons.

To test associations between survival modes and climate variables, we calculated the MAT[17] (MAT), the MAP[17] and mean CWD for each plot (1901–2013)[17]. As a metric of aridity, annual CWD (mm yr^{-1}) was calculated as the sum of monthly deficit values, which is the difference between potential and actual evapotranspiration[48,53]. Because the response variable, the relative abundance of the survival mode on a plot, was a percentage bounded at 0 and 100, multiple Tobit regression models were run with backwards selection using the vglm function in the VGAM package[54] in R on MAT, MAP and CWD. Residual diagnostics indicated that the Palamanui plot data was an outlier and was subsequently removed from the analysis of climate relations; none of the remaining plots data had undue leverage on the regression. The best fit model by Akaike Information Criterion (AIC) corrected for the small sample size of plots (AICc) contained MAT and CWD as significant predictors (Supplemental Table 6).

We compared observed changes in biomass at each plot with changes predicted from projecting each survival mode forward using an IBM parameterized with mean and 95% parameters for each survival mode. For example, stems were assigned a survival mode and each year grew and survived with probabilities corresponding to the 95th percentile growth rate and the size-dependent survival curve of that mode. Each survival mode population in the IBM was initialized with the size distribution in the first census at the respective site and then projected forward in time for the length of the census interval at each site. At the end of the projection, we calculated the biomass in each survival mode based on the mean wood density of each mode. We used the 95th percentile of growth rates by survival mode in the model to best capture canopy tree growth rates that are the greatest contributors to biomass. We also present the results using mean growth rate for comparison (Supplementary Fig. 11). Biomass was calculated as above using the mean wood density of each survival mode rather than species-specific values.

Reporting Summary

Further information on experimental design is available in the Nature Research Reporting Summary linked to this article.

Data availability

The data supporting the findings of this study are available from https://forestgeo.si.edu/climate-sensitive-size-dependent-survival-tropical-trees.

References

1. Bonan, G. B. Forests and climate change: forcings, feedbacks, and the climate benefts of forests. Science 320, 1444–1449 (2008). 2. Pan, Y. et al. A large and persistent carbon sink in the world's forests. Science 333, 988–993 (2011). 3. Wright, S. J. Te carbon sink in intact tropical forests. Glob. Change Biol. 19, 337–339 (2013). 4. Brienen, R. J. W. et al. Long-term decline of the Amazon carbon sink. Nature 519, 344–348 (2015).

5. Allen, C. D., Breshears, D. D. & McDowell, N. G. On underestimation of global vulnerability to tree mortality and forest die-of from hotter drought in the Anthropocene. Ecosphere 6, 1–55 (2015). 6. Friend, A. D. et al. Carbon residence time dominates uncertainty in terrestrial vegetation responses to future climate and atmospheric CO2. Proc. Natl Acad. Sci. USA 111, 3280–3285 (2014). 7. McMahon, S. M., Parker, G. G. & Miller, D. R. Evidence for a recent increase in forest growth. Proc. Natl Acad. Sci. USA 107, 3611–3615 (2010). 8. van der Sande, M. T. et al. Abiotic and biotic drivers of biomass change in a Neotropical forest. J. Ecol. 105, 1223–1234 (2017). 9. Johnson, M. O. et al. Variation in stem mortality rates determines patterns of above-ground biomass in Amazonian forests: implications for dynamic global vegetation models. Glob. Change Biol. 22, 3996–4013 (2016). 10. Chesson, P. Mechanisms of maintenance of species diversity. Annu. Rev. Ecol. Syst. 31, 343–366 (2000). 11. Adler, P. B., Ellner, S. P. & Levine, J. M. Coexistence of perennial plants: an embarrassment of niches. Ecol. Lett. 13, 1019–1029 (2010). 12. Purves, D. & Pacala, S. Predictive models of forest dynamics. Science 320, 1452–1453 (2008). 13. Coomes, D. A. & Allen, R. B. Mortality and tree-size distributions in natural mixed-age forests. J. Ecol. 95, 27–40 (2007). 14. Rees, M., Condit, R., Crawley, M., Pacala, S. & Tilman, D. Long-term studies of vegetation dynamics. Science 293, 650–655 (2001). 15. Cobb, R. C., Filipe, J. A. N., Meentemeyer, R. K., Gilligan, C. A. & Rizzo, D. M. Ecosystem transformation by emerging infectious disease: loss of large tanoak from California forests. J. Ecol. 100, 712–722 (2012). 16. Bennett, A. C., McDowell, N. G., Allen, C. D. & Anderson-Teixeira, K. J. Larger trees sufer most during drought in forests worldwide. Nat. Plants 1, 15139 (2015). 17. Anderson-Teixeira, K. J. et al. CTFS-ForestGEO: a worldwide network monitoring forests in an era of global change. Glob. Change Biol. 21, 528–549 (2015). 18. McDowell, N. et al. Drivers and mechanisms of tree mortality in moist tropical forests. New Phytol. 219, 851–869 (2018). 19. Hennig, C. Dissolution point and isolation robustness: robustness criteria for general cluster analysis methods. J. Multivar. Anal. 99, 1154–1176 (2008). 20. McFadden, D. in Frontiers in Economics (ed. Zarembka, P.) 105–142 (Academic Press, New York, 1973). 21. Vanclay, J. K. Mortality functions for North Queensland rain forests. J. Trop. For. Sci. 4, 15–36 (1991). 22. Rüger, N., Huth, A., Hubbell, S. P. & Condit, R. Response of recruitment to light availability across a tropical lowland rain forest community. J. Ecol. 97, 1360–1368 (2009). 23. Eichhorn, M. P., Nilus, R., Compton, S. G., Hartley, S. E. & Burslem, D. F. R. P. Herbivory of tropical rain forest tree seedlings correlates with future mortality. Ecology 91, 1092–1101 (2010). 24. Bell, T., Freckleton,

R. P. & Lewis, O. T. Plant pathogens drive densitydependent seedling mortality in a tropical tree. Ecol. Lett. 9, 569–574 (2006). 25. Packer, A. & Clay, K. Soil pathogens and spatial patterns of seedling mortality in a temperate tree. Nature 404, 278–281 (2000). 26. Chambers, J. Q., dos Santos, J., Ribeiro, R. J. & Higuchi, N. Tree damage, allometric relationships, and above-ground net primary production in central Amazon forest. For. Ecol. Manag. 152, 73–84 (2001). 27. Silver, E. J., Fraver, S., D'Amato, A. W., Aakala, T. & Palik, B. J. Long-term mortality rates and spatial patterns in an old-growth Pinus resinosa forest. Can. J. For. Res. 43, 809–816 (2013). 28. McDowell, N. G. & Allen, C. D. Darcy's law predicts widespread forest mortality under climate warming. Nat. Clim. Change 5, 669–672 (2015). 29. Meakem, V. et al. Role of tree size in moist tropical forest carbon cycling and water defcit responses. New Phytol. 219, 947–958 (2018). 30. Kraf, N. J. B., Metz, M. R., Condit, R. S. & Chave, J. Te relationship between wood density and mortality in a global tropical forest data set. New Phytol. 188, 1124–1136 (2010). 31. Poorter, L. Te relationships of wood-, gas- and water fractions of tree stems to performance and life history variation in tropical trees. Ann. Bot. 102, 367–375 (2008). 32. Wright, S. J. et al. Functional traits and the growth–mortality trade-of in tropical trees. Ecology 91, 3664–3674 (2010). 33. Poorter, H., Niinemets, Ü., Poorter, L., Wright, I J. & Villar, R. Causes and consequences of variation in leaf mass per area (LMA): a meta-analysis. New Phytol. 182, 565–588 (2009). 34. Westoby, M., Falster, D. S., Moles, A. T., Vesk, P. A. & Wright, I. J. Plant ecological strategies: some leading dimensions of variation between species. Annu. Rev. Ecol. Syst. 33, 125–159 (2002). 35. Kraf, N. J. B., Godoy, O. & Levine, J. M. Plant functional traits and the multidimensional nature of species coexistence. Proc. Natl Acad. Sci. USA 112, 797–802 (2015). 36. Kramer-Schadt, S., Revilla, E., Wiegand, T. & Grimm, V. Patterns for parameters in simulation models. Ecol. Model. 204, 553–556 (2007). 37. Dietze, M. C. et al. A quantitative assessment of a terrestrial biosphere model's data needs across North American biomes. J. Geophys. Res. Biogeosci. 119, 286–300 (2014). 38. Fisher, R. A. et al. Vegetation demographics in Earth System Models: a review of progress and priorities. Glob. Change Biol. 24, 35–54 (2018). 39. Condit, R. Tropical Forest Census Plots: Methods and Results from Barro Colorado Island, Panama and a Comparison with Other Plots (Springer Science & Business Media, New York, 1998). 40. R Development Core Team R: A language and Environment for Statistical Computing (R Foundation for Statistical Computing, Vienna, 2015). 41. Stan Development Team Stan: A C++ Library for Probability and Sampling v.2.10.0 (2015). 42. Marod, D., Kutintara, U., Yarwudhi, C., Tanaka, H. & Nakashisuka, T. Structural dynamics of a natural mixed deciduous forest in western Tailand. J. Veg. Sci. 10, 777–786 (1999). 43. Metcalf, C. J. E., Horvitz, C. C., Tuljapurkar, S. & Clark, D. A. A time to grow and a time to die: a new way to analyze the dynamics of size, light, age, and death of tropical trees. Ecology 90, 2766–2778 (2009). 44. Miura, M., Manabe, T., Nishimura, N. & Yamamoto, S. Forest canopy and community dynamics in a temperate old-growth evergreen broad-leaved

forest, south-western Japan: a 7-year study of a 4-ha plot. J. Ecol. 89, 841–849 (2001). 45. Needham, J., Merow, C., Chang-Yang, C. H., Caswell, H. & McMahon, S. M. Inferring forest fate from demographic data: from vital rates to population dynamic models. Proc. R. Soc. B 285, 2017–2050 (2018). 46. Lê, S., Josse, J. & Husson, F. FactoMineR: An R package for multivariate analysis. J. Stat. Sofw. 25, 1–18 (2008). 47. Husson, F., Josse, J. & Pages, J. Principal Component Methods-Hierarchical Clustering-Partitional Clustering: Why Would We Need to Choose for Visualizing Data Technical Report of the Applied Mathematics Department (Agrocampus Quest, Rennes, 2010). 48. Chave, J. et al. Improved allometric models to estimate the aboveground biomass of tropical trees. Glob. Change Biol. 20, 3177–3190 (2014). 49. Chave, J. et al. Towards a worldwide wood economics spectrum. Ecol. Lett. 12, 351–366 (2009). 50. Swenson, N. G. et al. Temporal turnover in the composition of tropical tree communities: functional determinism and phylogenetic stochasticity. Ecology 93, 490–499 (2012). 51. Zanne, A. E. et al. Global Wood Density Database (Dyrad Digital Repository, 2009); https://doi.org/10.5061/dryad.234. 52. Katabuchi, M., Kurokawa, H., Davies, S. J., Tan, S. & Nakashizuka, T. Soil resource availability shapes community trait structure in a species-rich dipterocarp forest. J. Ecol. 100, 643–651 (2012). 53. Stephenson, N. L. Climatic control of vegetation distribution: the role of the water balance. Am. Nat. 135, 649–670 (1990). 54. Yee, T. W. Te VGAM package for categorical data analysis. J. Stat. Sofw. 32, 1–34 (2010).

Acknowledgements

The authors thank the many people involved in establishing and maintaining all the plots utilized in these analyses. A detailed list of funding sources for each plot is available in the Supplementary Information. The development of this project benefited from ForestGEO workshops in 2015, 2016 and 2017 (NSF DEB-1046113 to S.J.D.). Contributions by C.X., J.Q.C., S.J.D. and N.M. were supported by the Next-Generation Ecosystem Experiments (NGEE-Tropics) project, funded by the US Department of Energy, Office of Biological and Environmental Research. S.M.M. was partially funded by NSF - EF1137366. D.J.J. was supported by Los Alamos National Laboratory (Director’s Post-doctoral Fellowship).